Origin of Tokamak Density Limit Scalings

D. A. Gates and L. Delgado-Aparicio

Phys. Rev. Lett. **108**, 165004 — Published 20 April 2012

DOI: 10.1103/PhysRevLett.108.165004

On the origin of tokamak density limit scalings*

D. A. Gates, L. Delgado-Aparicio

Plasma Physics Laboratory, Princeton University, P.O.Box 451,

Princeton, New Jersey 08543

Abstract

The onset criterion for radiation driven islands [Rebut and Hugon, Plasma Physics and Controlled Nuclear Fusion Research 1984 (Proc. 10th Int. Conf. London, 1984), Vol. 2, IAEA, Vienna, 197, (1985)] in combination with a simple cylindrical model of tokamak current channel behavior is consistent with the empirical scaling of the tokamak density limit [Greenwald, Nucl. Fusion **28** (1988) 2199]. Many other unexplained phenomena at the density limit are consistent with this novel physics mechanism.

The empirical scaling of the density limit in tokamaks has long been known and is a surprisingly robust experimental result. Whereas the exact form of the scaling law evolved over decade long international experimental activities [1, 2, 3, 4, 5, 6], the physics mechanism for the onset of the density limit, which has come to be known as the Greenwald limit after the author of reference [3], has remained elusive. The phenomenology has been described in great detail (for an excellent review of the experimental observations see [4]). The onset of the plasma collapse associated with this empirical limit is associated with both the radiative collapse of the current profile and the appearance of one or more low order magnetic islands. The phenomenology is apparently universal.

A list of unexplained phenomena are associated with the density limit:

1) The scaling is universal, but the phenomenon appears associated with radiative collapse which can be complicated given the quantum nature of impurity line radiation.

2) If the physics is associated with radiative collapse, why is the density limit so weakly dependent on heating power?

3) Why is the limit only weakly dependent on the type of radiator?

4) The collapse is associated with the onset of magnetic islands, so why

does the limit not depend on plasma shaping or q (both which are known to affect MHD stability)?

5) Why is the density limit power scaling different in stellarators?

6) Why are tearing modes associated with the radiative collapse?

We put forward and analyze the basic hypothesis that radiation driven islands, described first in [7], are the cause of the density limit. The association between radiation driven islands and the density limit is not new. In fact, the possibility of the islands occurring at the density limit being radiation driven is discussed at length in an experimental context on the ASDEX-U tokamak by Suttrop in Reference [8], however the possibility of a causal relationship was not considered. An important additional step in understanding radiative islands was taken in Reference [9] when a radiative term was added to the Modified Rutherford Equation [10] and the time dependence of island growth at the density limit was analyzed. However, this work also did not claim a causal link between radiative islands and the Greenwald limit. The theory of radiative islands was further expanded and formalized, where an additional term is added to the modified Rutherford Equation, and shown to be consistent with the early appearance of NTMs in NSTX [11]. Observations of the tearing phase of snake modes on Alcator C-Mod tokamak [12]

have also been associated with radiative drive. The onset criteria for the effect is easily understood: the interior region of an island contains impurities, the impurities radiate cooling the island interior, thereby increasing the local resistivity, thus the helical current perturbation is increased causing the island to grow. A key additional observation is that the interior of the island is shielded from any auxiliary heating power that is deposited in the core of the device, being shunted around the island by heat conduction parallel to the magnetic field. At this point, it becomes clear why such a process would not occur in stellarators. In stellarators, the equilibrium is determined by external coils. This means that a perturbation to the equilibrium magnetic field due to the inductively driven plasma current is not possible, because there is no inductively driven current. Thus in stellarators added heating power raises the density limit like $P^{1/2}$ as would be expected from global power balance. The situation for a tokamak island is shown schematically in Figure 1. The problem of heat conduction around a thin island is handled in detail in Referenc [13]. We imagine a scenario where an island of small but finite size has been created by a perturbation. Because it is shielded from the auxiliary heating sources, which are typically centrally peaked, the stability criterion for radiative driven islands of the island interior is expressed as a

constraint on the radiated power and the ohmic power such that:

$$P_{rad} < \eta J^2 \tag{1}$$

which we rewrite:

$$E_{eff}\nu_{eZ_{eff}} n_e < \frac{m_e \nu_{ei}}{e^2 n_e} J^2 \tag{2}$$

where E_{eff} is the energy lossed per excitation collision summed over all radiating lines, $\nu_{eZ_{eff}}$ is the effective collision frequency for radiative collisions, n_e is the electron density, m_e is the electron mass, ν_{ei} is the electron-ion collision frequency, e is the electron charge, and J is the local current density with all quantities evaluated at the rational surface of interest. This expression can be rewritten as:

$$n_e < \sqrt{\frac{m_e}{e^2 E_{eff}} \frac{\nu_{ei}}{\nu_{eZ_{eff}}}} J \quad or \quad n_e < f(Z, T_e) J \tag{3}$$

This is suggestive of the Greenwald limit [3] which is written

$$\overline{n}_e < \frac{I_p}{\pi a^2} \tag{4}$$

where $\bar{n_e}$ is the line averaged (as from an interferometer) electron density, I_p is the total plasma current, and a is the plasma geometric minor radius.

The difference between Equation 3 and Equation 4 being the island onset criterion is given in terms of local parameters where as the Greenwald limit is in terms of global parameters.

It is appropriate to discuss in some detail the term under the radical in Equation 3. It turns out the realization that the balance described by Equation 1 gives scaling laws similar to the Greenwald limit is also not new. In fact there are many papers proposing this type of balance, all of which considered balancing radiative loss against the ohmic heating in some region of the plasma cross-section (see, for example, [16, 17]). Most of these were not considered seriously as explanations of the density limit because they do not explain the fact that density limit does not increase as $P_{aux}^{1/2}$. However, the detailed ohmic vs. radiative power balance calculations have been done previously. In particular, reference [16] shows that over a wide region which covers most of the existing tokamak database, the ratio of the radiated power to the ohmic input power is very nearly independent of plasma temperature.

To relate the local parameters of Equation 3 and global parameters of Equation 4 we consider a family of current profiles of the form:

$$J = \frac{J_0}{\left(1 + \left(\frac{r}{r_0}\right)^{2\nu}\right)^{1+\frac{1}{\nu}}} \tag{5}$$

As ν increases, the profiles go from peaked to flat, representing a typical collapsed current profile for large values of ν. This class of profiles was first used in Reference [14]. Additionally we assume a parabolic density profile. A representative set of current profiles at fixed edge-q is shown in Figure 2. Each curve has J_0 chosen such that $q_0 = 0.9$, consistent with the observation that the peak current density inside the $q = 1$ rational surface saturates due to the $m/n = 1$ instability (aka the sawtooth instability).

To understand where the Greenwald limit lies in this space we first plot contours of constant total plasma current versus the free profile parameters ν and r_0 (shown in Figure 3). Additional information is required to locate the density limit. In particular, since it is well established the current profile peaks as the density limit is approached, a measure of the current profile peaking for each value of the plasma current is required. The required information is taken from a plot from Reference [15]. Figure 6 of this reference shows the operational boundary for the JET tokamak as a function of q_{edge} and l_i. The upper bound of this plot represents the density limit. The limit

is parameterized with a linear fit given by:

$$l_i = 0.12 * q_{edge} + .6 \tag{6}$$

where l_i is the normalized internal inductance of the plasma (as defined in reference [15]). The contour of the fit curve given by Equation 6 is shown in Figure 3. We note here that for plasmas with high internal inductances as described by the relationship above, plasma boundary shaping does not have a strong effect on the low order rational surfaces so that the shape of these surfaces will be roughly circular. This is a plausible explanation as to why plasma shaping does not affect the Greenwald limit. We also note that the experimentally observed current profile peaking at the density limit corresponds to the knee in the constant q contours where the main variation in the profile parameters changes from strongly varying r_0 to strongly varying ν. This corresponds to the point where the bulk of the (fixed) plasma current is now inside the q=1 surface. further increase in l_i from this point lead to rapid reductions in the current density outside the $q = 1$ surface. This behavior is important in understanding the relationship between the average current density (as appears in the Greenwald limit Equation 4) and the current density at a local surface as given in Equation 3.

The next step is to see if the local criterion due to the onset of a radiation driven island actually corresponds with the Greenwald limit. In other words, along the contour that represents the current profiles for the density limit in Figure 3 there should be a correlation with the following expressions

$$\frac{f(Z)J(r_{m/n})}{n_e(r_{m/n})} = \frac{I_p}{\overline{n}_e \pi a^2} \tag{7}$$

The assumption of a parabolic density profile $n(r) = n(0)(1 - (r/a)^2)$ gives

$$\frac{J(r_{m/n})}{I_{tot}(1 - \frac{r^2_{m/n}}{a^2})} = \frac{n_e(0)}{\overline{n}_e} \frac{1}{f(Z)\pi a^2} \tag{8}$$

where the term on the right is constant for the purposes of this discussion.

As an example, the contour of the expression above for the $q = 2$ surfaces as determined by the profile model is shown in blue in Figure 3. The agreement between the observed experimentally determined current profile behavior and the behavior of the radiation driven onset criterion is remarkable given the simplicity of the model used to describe the profile behaviors.

The final step is an evaluation of the numerical coefficients in Equation 8. All quantities are known except the numerical factor $f(Z)$ which is defined in Equation 3. The variables are reformulated according to the cooling rate

expression given in Reference [18], which assumes coronal equilibrium. The ion-electron collision frequency is taken from the NRL plasma formulary [19]. The expression then becomes:

$$f(Z) = \sqrt{\frac{3.26x10^{-9} n_D \ln \Lambda_D \left(1 + \sum_{i=2}^{n} \alpha_{z_i}\right)}{T_e^{3/2} \sum_{i=1}^{n} n_{z_i} L_{z_i}}} \tag{9}$$

where L_{z_i} is the cooling rate of the ith impurity from Reference [18], $\ln \Lambda_D$ is the Coulomb logarithm for the main species assumed to be Deuterium, α_{z_i} is the impurity impact strength factor defined as $Z_i^2(n_Z/n_D)$. Assuming the following parameters: single impurity species is Carbon, $n_C/n_D \sim 5.5\%$, $T_e = 1$keV, $\ln \Lambda_D = 15$ and using $L_C = 10^{-35}(Wm^3)$ and with the fraction on the left side of Equation 8 set to 3 as determined from the contour plot in Figure 3 yields:

$$\frac{f(Z)\pi a^2 J(r_{m/n})}{I_{tot}(1 - \frac{r_{m/n}^2}{a^2})} \frac{\overline{n}_e}{n_e(0)} \sim 1.7 \tag{10}$$

compared to an expectation of unity. Given the limitations of the model and example employed this is surprisingly good agreement.

This model is consistent with all the unexplained phenomena presented above. It also is consistent with detailed analysis of phenomenology of density limit disruptions described in numerous publications. Of particular note are:

1) the cold bubble formation described in [20], which may be caused by a 1/1 radiation driven island,

2) the loss of confinement near the density limit [4], which could be due to the onset of stochasticity in the presence of multiple islands

3) the ability to exceed the density limit by profile peaking, which would not affect the density at the 2/1 surface [21]

4) the doubling of the density limit in helium observed in Reference [22] likely a direct result of the collisionality scaling of Equation 3 assuming fixed impurity densities

There are two important factors that make this potentially complex phenomena exhibit such a simple scaling behavior; the clamping of the the central current density inside the $q = 1$ surface forces the q=1 radius to grow and the profile develops a top-hat like distribution and, as discussed previously, the ratio of ohmic heating to the total radiation is nearly independent of plasma temperature, over a wide range of parameters.

One obvious prediction of this work is that direct heating of the rational surfaces that participate in the radiation driven island phenomena should suppress these islands, since this would avoid the shielding process described above. Operating above the density limit could be important for burning

tokamaks, such as ITER [23]. In fact this result may have already been demonstrated in experiments, such as in References [24, 25]. For future tokamaks, which may operate at higher temperature and density, bremsstrahlung radiation may become dominant giving a lower density limit. Additionally, radiation driven islands should be exacerbated in plasmas with high non-inductive current fractions, since only the ohmic current participates in heating the interior of the island. This may explain the common practice of using "preventative ECRH" to avoid the onset of neoclassical tearing modes. In fact this phenomenon may partially explain the difficulty in finding a reliable predictor for the onset of neoclassical tearing modes because the radiation driven terms are not considered in neoclassical island threshold analysis [26]. It is hoped that given the apparent success of this simple model in explaining the observed global scalings will lead to a more comprehensive analysis of the possibility that radiation driven islands are the physics mechanism responsible for the density limit. In particular, with modern diagnostic capabilities detailed measurements of current densities, electron densities and impurity concentrations at rational surfaces should be possible, enabling verification of the mechanism described above.

The first author would like to acknowledge helpful discussions with R. B. White and

W. Suttrop, and also J. Hugill for describing the mysterious behavior of the tokamak density limit.

*This work was supported by the U.S. Department of Energy Grant under contract number DE-AC02-76CH03073.

References

[1] M. Murakami, J. D. Callen, L. A. Berry, Nucl. Fusion **16** (1976) 347.

[2] S.J. Fielding, J. Hugill, G.M. McCracken, J.W.M. Paul, R. Prentice, P.E. Stott, Nucl. Fusion **17** (1977) 1382

[3] M. Greenwald, J.L. Terry, S.M. Wolfe S. Ejima, M.G. Bell, S.M. Kaye, G.H. Neilson, Nucl. Fusion **28** (1988) 2199.

[4] M. Greenwald, Plasma Phys. Control. Fusion **44** (2002) R27.

[5] R. Granetz, Phys. Rev. Lett. **49** (1982) 658.

[6] E.S. Marmar, J. E. Rice, J. L. Terry, F. H. Sequin, Nucl. Fusion **22** (1982) 1567.

[7] P. H. Rebut and M. Hugon, Plasma Physics and Controlled Nuclear Fusion Research 1984 (Proc. 10th Int. Conf. London, 1984), Vol. 2, IAEA, Vienna, 197, (1985).

[8] W. Suttrop, K. Buchl, J.C. Fuchs, M. Kaufmann, K. Lackner, et al., Nucl. Fusion, **37** (1997) 119.

[9] F. Salzedas, F. C. Schuller, A.A.M. Oomens, and the RTP Team, Phys. Rev. Lett. **88** (2002) 075002-1.

[10] P. H. Rutherford, PPPL Report 2277, (1985).

[11] L. Delgado-Aparicio, D. Stutman, K. Tritz, F. Volpe, K.L. Wong, et al., Nucl. Fusion **51** (2011) 083047.

[12] L. Delgado-Aparicio, to be submitted to Phys. Rev. Lett. 2012.

[13] R. Fitzpatrick, Phys. Plasmas **2** (1995) 825.

[14] H. P. Furth, P. H. Rutherford, and H. Selberg, Phys. Fluids **16** (1973) 1054.

[15] J. A. Wesson, R. D. Gill, M. Hugon, F. C. Schuller, J. A. Snipes, et al., Nucl. Fusion **29** (1989) 641.

[16] F. W. Perkins and R. A. Hulse, Phys. Fluids **28** (1985) 1837.

[17] W. M. Stacey, Phys. Plasmas **4** (1997) 1069.

[18] D. E. Post, R. V. Jensen, C. B. Tarter, W. H. Grassberger, W. A. Lokke, At. Data Nucl. Data Tables **20** (1977) 397

[19] NRL Plasma Formulary, (2011) available online at `http://wwwppd.nrl.navy.mil/nrlformulary/`

[20] J. Howard and M. Persson, Nucl. Fusion **32** 1992 361.

[21] Y. Kamada, N. Hosogane, R. Yoshino, T. Hirayama, T. Tsunematsu Nucl. Fusion, **31** (1991) 1827.

[22] J. Rapp, A. Huber, L.C. Ingesson, S. Jachmich, G.F. Matthews, et al., J. Nucl. Mater. **313-316** (2003) 524

[23] ITER Physics Basis, Nucl. Fusion **39** (1999)

[24] F. Salzedas, A.A.M. Oomens, R.W. Polman, F.C. Schuller and the RTP team, In *Proceedings of 25th EPS Conference on Controlled Fusion and Plasma Physics Praha*, June, 1998 available online at `http://epsppd.epfl.ch/Praha/WEB/98ICPP_W/B019PR.PDF`

[25] B. Esposito G. Granucci, P. Smeulders, S. Nowak, J. R. Martin-Solis, L. Gabellieri, et al., Phys. Rev. Lett. **100** (2008) 045006

[26] D. A. Gates, B. Lloyd, A. W. Morris, G. McArdle, M. R. O'Brien, et al., Nucl. Fusion **37** (1997) 1593.

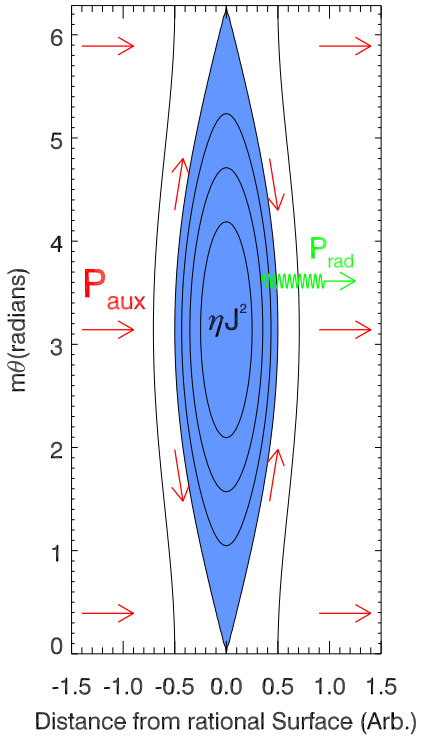

Figure 1: Representation of single lobe of a magnetic island schematically showing the heat flow from the auxiliary heating around the island (red arrows), the resistive heating inside the island (blue area), and the radiation losses from within the island interior (green arrow).

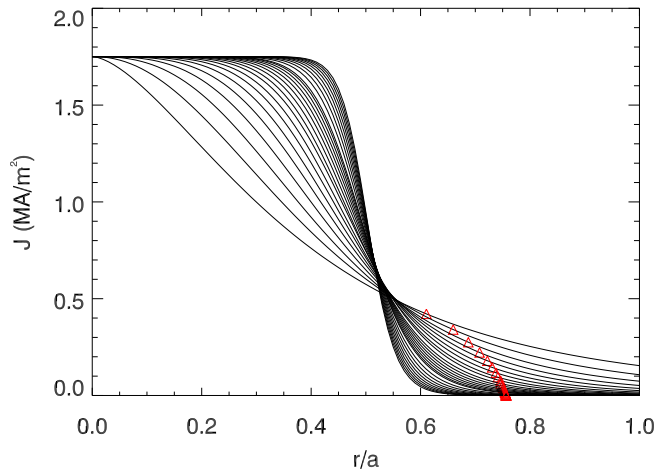

Figure 2: Plot of the family of current density curves used for the density limit model. This set of curves have constant $q_{edge} = 3.5$. The red triangles indicate the position of the q=2 surface for each profile.

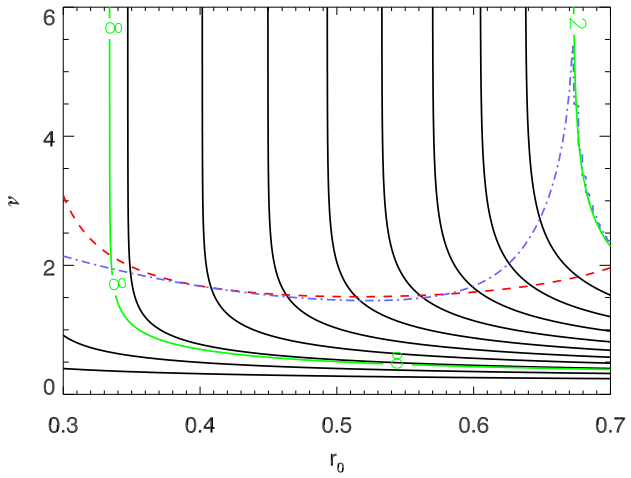

Figure 3: Contour plot of the total plasma current (black) as a function of the profile parameters ν and r_0. Also shown in the plot are the contour of the current profile peaking at the density limit as given by Equation 6 (red) and the best fit contour of the quantity from Equation 8 (blue). The green curves show the location of $q_{edge} = 2$ and $q_{edge} = 8$ for reference (contour labels indicate q_{edge} values).